Investigation on thermal characteristics of novel composite sorbent with carbon coated iron as additive

L. Jiang[a,b,*], R.Z. Wang[b], A.P. Roskilly[a]

[a]*Sir Joseph Swan Centre for Energy Research, Newcastle University, Newcastle NE1 7RU, UK*

[b]*Institute of Refrigeration and Cryogenics, Shanghai Jiao Tong University, Shanghai, 200240, China*

Abstract: Carbon coated iron and expanded natural graphite are selected as the additives in developing novel consolidated composite strontium chloride, which is attempted to improve heat and mass transfer performance. Due to anisotropic characteristics, both disk and plate samples are investigated which are parallel and perpendicular to compression direction respectively. It is worth noting that thermal conductivity of composite sorbent increases with the increase of density and the decrease of mass ratio whereas permeability shows a reverse trend. Results demonstrate that the highest thermal conductivity of composite strontium chloride with carbon coated iron could reach 2.95 $W \cdot m^{-1} \cdot K^{-1}$, which is improved by 14 times when compared with granular salt. Permeability of composite sorbent ranges from 1.2×10^{-9} m^2 to 4.5×10^{-14} m^2 when density is in the range between 400 $kg \cdot m^{-3}$ and 600 $kg \cdot m^{-3}$. Sorption characteristic of composite sorbent with carbon coated iron is also investigated and compared with that not adding carbon coated iron. Under the condition of -10°C evaporation temperature, sorption reaction rate of composite sorbent with carbon coated iron is better than that without carbon coated iron due to the improved mass transfer performance. Sorption rates of composite sorbents are almost the same when evaporation temperature reaches 10°C.

Keywords: Composite sorbent, Carbon coated iron, Expanded natural graphite, Thermal conductivity

** Corresponding author. Tel. +86-21-34206309/44-07592206270*

Email: maomaojianglong@sjtu.edu.cn/Long.jiang@newcastle.ac.uk(L. Jiang)

Nomenclature

A	Area of cross section (m^2)
Al@C	Carbon coated aluminum
B	Shape factor
C	Specific heat ($J \cdot g^{-1} \cdot K^{-1}$)
EDX	Energy dispersive x-ray
ENG	Expanded natural graphite
ENG-TSA	Expanded natural graphite treated with sulfuric acid
Fe@C	Carbon coated iron
GF	Graphite flake
K	Permeability (m^2)
m	Mass flow rate ($kg \cdot s^{-1}$)
MWCNT	Multi-walled carbon nanotube
Ni@C	Carbon coated nickel
P	Pressure (Pa)
q	Gas volume flow rate ($L \cdot min^{-1}$)
R	Gas constant ($J \cdot mol^{-1} \cdot K^{-1}$)
SCP	Specific cooling power ($W \cdot kg^{-1}$)
SEM	Scanning electron microscopy
T	Temperature (^oC)
TES	Thermal energy storage
t	Time (s)
V	Axial velocity ($kg \cdot s^{-1}$)
x	Sorption capacity ($kg \cdot kg^{-1}$)

Greek letters

α	Thermal diffusivity ($mm^2 \cdot s^{-1}$)
β	Mass ratio of ENG
γ	Mass ratio of Fe@C
λ	Thermal conductivity ($W \cdot m^{-1} \cdot K^{-1}$)

μ	Gas viscosity (Pa·s)
ρ	Density (kg·m^{-3})
v’	Specific volume of saturated liquid ammonia (m^3·kg^{-1})
v”	Specific volume of saturated vapor ammonia (m^3·kg^{-1})
v	Sorption rate (kg·kg^{-1}·s^{-1})

Subscripts

a	Axial
c	Cross section
con	Condensation
de	Desorption
e	Evaporation
in	Inlet
max	Maximum
out	Outlet
$SrCl_2$	Strontium chloride
sorb	Sorbent

1. Introduction

Sorption reaction process is regarded as one of the most prospective approaches for low grade heat utilization due to its various applications of refrigeration [1, 2], heat pump [3, 4], power generation [5, 6], thermal energy storage (TES) [7, 8], carbon capture [9], desalination [10], etc. An eternal challenge is how to further realize desirable heat and mass transfer performance [11], which will have a great influence on sorption characteristic [12]. To address this problem, a main solution depends on the improvement of sorption reactor which consists of heat and mass transfer enhancement of heat exchanger and sorbent [13].

Various researches have been investigated to intensify heat transfer of heat exchanger by increasing heat transfer areas of finned tube [14]. Nonetheless, the larger heat transfer area inevitably increases thermal capacity which results in a low system efficiency [15]. In fact, heat transfer enhancement of heat exchanger has a limited improvement on sorption reactor due to the fact that the largest thermal resistance lies in sorbent side [16]. Therefore, heat and mass transfer enhancement of sorbent is essential for sorption systems. It is extensively acknowledged that composite sorbent is an effective method for heat and mass transfer intensification. Different matrices such as expanded natural graphite (ENG) [17], vermiculite [18, 19] and carbon nanoparticle [20] have been selected as the additives in developing composite sorbents. Among them, ENG has been widely investigated which could be classified into different types in term of its intercalation compound. Considering ENG without intercalation compound, early study of composite sorbent was carried out by Mauran et al. Results indicated that ENG could improve heat transfer of metal chloride [21]. Later, Tamainot-Telto et al. investigated thermal conductivity of composite sorbent by mixing activated carbon and ENG, and analysed its possible application for sorption refrigeration and heat pump [22, 23]. Jiang et al. [24, 25] evaluated thermal conductivity and permeability of eight different metal chlorides with ENG, and compared their properties in the sorption process. As for ENG with intercalation compound, expanded natural graphite treated with sulfuric acid (ENG-TSA) is quite representative, and sulphuric acid is adopted as graphite intercalation compound in the exfoliation process to obtain a lower density [26, 27]. Jiang et al. developed composite $CaCl_2$ with ENG-TSA as matrix. Results demonstrated that the highest thermal conductivity was able to reach 88.1 $W \cdot m^{-1} \cdot K^{-1}$ while permeability decreased to the magnitude of 10^{-14} m^2 [28]. One remarkable fact is that ENG is a good additive to improve heat transfer performance of the sorbent whereas mass transfer is slightly weakened.

Vermiculite has been verified to improve mass transfer performance of composite sorbent. However, heat transfer is not able to be further improved by using vermiculite as matrix since it has a relatively low thermal

conductivity [29]. In recent years, carbon nanoparticles are expected to improve heat transfer performance due to its distinguished characteristic. Yan et al. investigated sorption performance of multi-walled carbon nanotubes (MWCNT) and revealed that MWCNT could be selected as an additive for metal chlorides in the development of composite sorbent [30]. After that, a novel composite $CaCl_2$ with MWCNT as matrix was developed for investigating thermal conductivity and sorption kinetic. Results indicated that MWCNT was conducive to mass transfer performance with a limited improvement for thermal conductivity [31]. Comparably, carbon coated metal is also investigated for developing composite sorbent because of its wrapped structure. Carbon coating protects external condition for metal inside with excellent thermo-physical properties remained, which could prevent serious swelling and agglomeration in mass transfer process [32, 33]. Since ENG and carbon nanoparticles have respective influence on granular sorbent, it tends to consider a coupling enhancement of composite sorbent by using both of the additives. Our previous work verified that additives of ENG and carbon coated aluminum (Al@C) had a positive influence on heat and mass transfer performance of sorbent [34]. Nonetheless, various carbon coated metals have a different influence on heat and mass transfer of sorbents. This may result in a diversity of sorption and desorption performance, which could be used for different applications.

This paper aims to further investigate novel composite $SrCl_2$ which is impregnated with ENG and carbon coated iron (Fe@C). Composite sorbents with different matrices i.e. carbon coated nickel (Ni@C), Al@C and Fe@C are comprehensively compared and analyzed in term of heat and mass transfer performance. Also sorption characteristic is investigated and analyzed based on the improved heat and mass transfer performance.

2. Development of novel composite $SrCl_2$

Thermochemical reaction process of $SrCl_2$ with ammonia could be according to equations 1-2. Table 1 indicates the main parameters of $SrCl_2$ in term of equilibrium desorption temperature, molar mass, maximum

cycle sorption capacity, thermal conductivity and permeability, reaction enthalpy and entropy. To simplify the description of chemisorption process of $SrCl_2$, phrase of $SrCl_2$ 8/1 is used in the rest of this paper, which represents that $SrCl_2$ ammoniate reacts with ammonia from 1 mole to 8 moles. As for reaction process from 0 mole to 1 mole, it is difficult to be used in general temperature range of low grade heat i.e. lower than 300°C.

Table 1. The main parameters of granular $SrCl_2$.

Sorbent	$SrCl_2$ 8/1
Equilibrium desorption temperature (°C)	96 (30°C condensation temperature)
Molar mass ($g \cdot mol^{-1}$)	158.4
Reaction enthalpy ΔH ($J \cdot mol^{-1}$)	41432
Reaction entropy ΔS ($J \cdot mol^{-1} \cdot K^{-1}$)	228.6
Maximum cycle sorption capacity Δx_{max} ($kg \cdot kg^{-1}$)	0.75
Thermal conductivity ($W \cdot m^{-1} \cdot K^{-1}$)	0.21
Permeability (m^2)	10^{-9}

$$SrCl_2 \cdot NH_3 + 7NH_3 \longleftrightarrow SrCl_2 \cdot 8NH_3 + 7\Delta H_{SrCl_2} \quad (1)$$

$$NH_3(gas) \longleftrightarrow NH_3(liq) + \Delta H_{con} \quad (2)$$

ENG is beforehand expanded by the optimal expanding process, i.e. heating expandable natural graphite in an oven at the temperature of 600°C for 8 minutes [35]. Detailed developing processes of novel composite $SrCl_2$ with ENG and Fe@C are illustrated in Fig.1. First, Fe@C is dispersed with ethanol in ultrasonic bath for 30 minutes to prevent the aggregation (a_1 process). Meanwhile, $SrCl_2$ is stirred and dissolved in the water (a_2 process). Then ENG is dried in an oven at a controlled temperature of 120°C for two hours. ENG, Fe@C and $SrCl_2$ solution are stirred and mixed together in ultrasonic bath for another 30 minutes (b process). After that, the mixture will be dried in an oven at 160°C for 48 hours (c process). Composite sorbent is developed, and it will be

put into a vessel and pressed by compressing machine (d process). Finally, consolidated composite sorbent will be transferred into sample mold for testing (e process).

Considering our previous work of composite $SrCl_2$ with ENG and Al@C, crack easily happens if density is lower than 400 $kg \cdot m^{-3}$, which brings about poor mechanical stability of composite sorbent. Similar with our previous work, density of novel composite $SrCl_2$ with ENG and Fe@C is selected in the range from 500 $kg \cdot m^{-3}$ to 800 $kg \cdot m^{-3}$ which is suitable for comparison. Mass ratio between $SrCl_2$ and ENG ranges from 50% to 83% i.e. from 1:1 to 5:1 whereas mass ratio between ENG and Fe@C is adopted as 20:1 [36]. Bulk density of ENG is indicated in Fig.2 which is calculated by dividing the whole volume with mass of ENG. It is worth noting that bulk density of ENG is in the range from 85 $kg \cdot m^{-3}$ to 392 $kg \cdot m^{-3}$. For comparing anisotropic characteristics, both disk and plate samples are developed i.e. heat and mass transfer testing direction are parallel and perpendicular to compression direction, respectively.

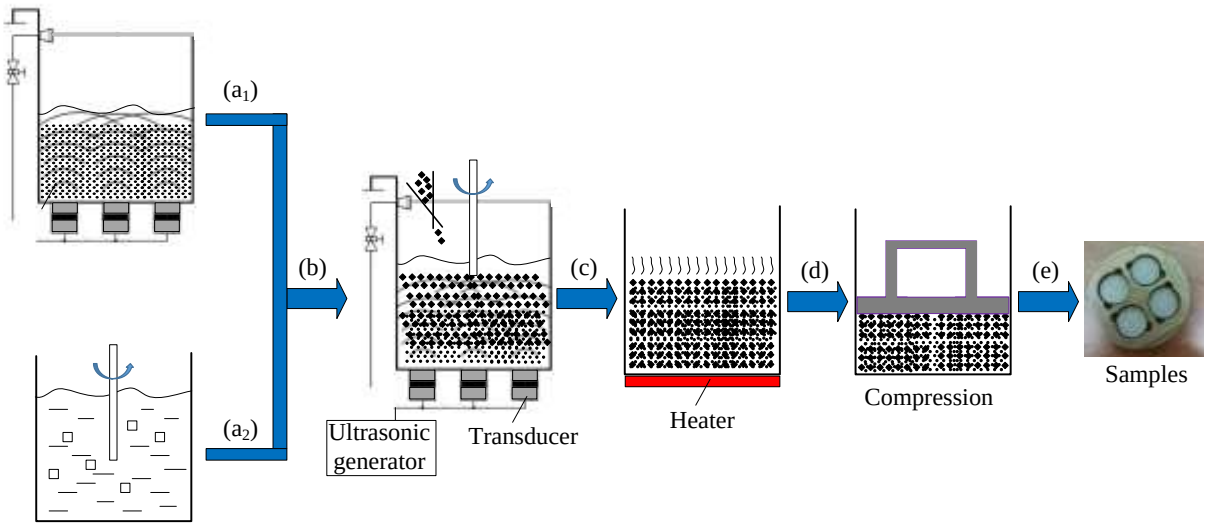

Fig.1. Developing process of novel composite $SrCl_2$ with ENG and Fe@C.

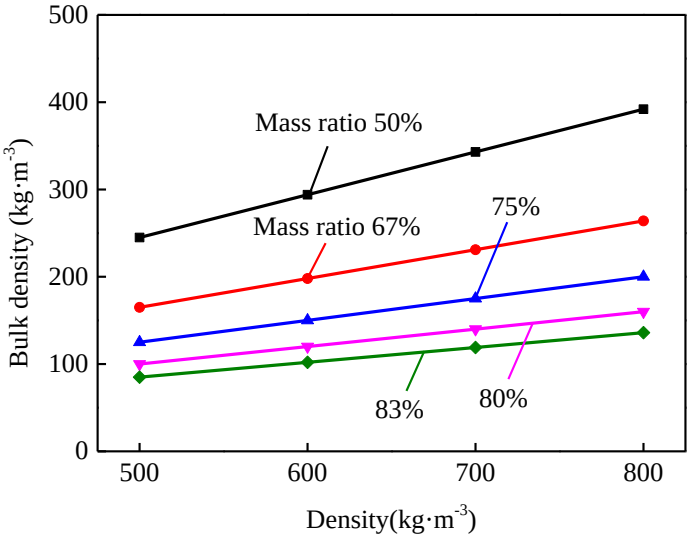

Fig.2. Bulk density of ENG vs. density of novel composite $SrCl_2$ with ENG and Fe@C.

Fig.3 demonstrates SEM image and EDX mapping of novel composite $SrCl_2$ with ENG and Fe@C which is used to further observe microscale characteristic. Fig.3a demonstrates SEM image of composite $SrCl_2$, which illustrates its surface morphology. Fig.3b and Fig.3c show the distribution of element Fe and Cl, which reveals the uniformity of Fe@C and $SrCl_2$.

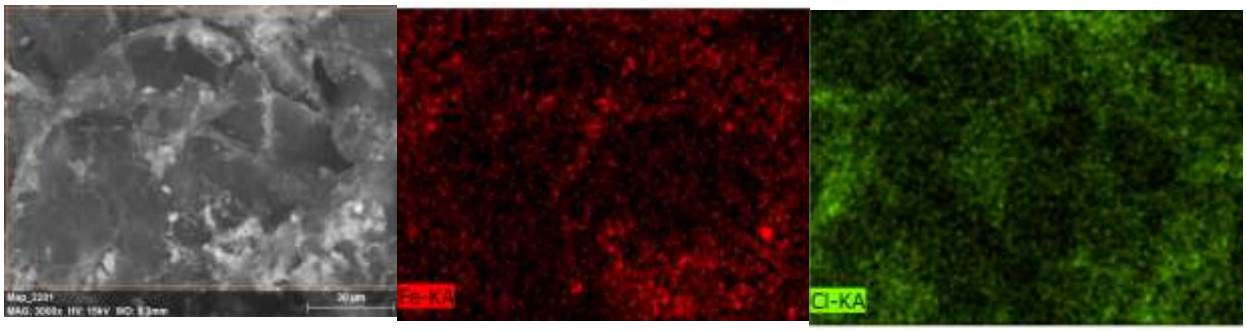

(a) (b) (c)

Fig.3. SEM image and EDX mapping of novel composite $SrCl_2$ (a) SEM; (b) EDX mapping of element Fe; (c) EDX mapping of element Cl.

3. Testing methodology

The detailed testing procedures of heat and mass transfer performance could refer to our previous work [34]. Thermal conductivity of novel composite sorbent is investigated by laser flash method, and the concerning testing unit is LFA467 instrument in this experiment. Under this scenario, thermal conductivity is evaluated by equation 3, which is a product of thermal diffusivity, specific heat and density. Thermal diffusivity is determined by half temperature rising curve. The random error of this testing equipment is less than 0.1%, and the largest relative error of thermal conductivity is 5%.

$$\lambda(T) = \alpha(T)\cdot C_p(T)\cdot \rho(T) \tag{3}$$

where $\lambda(T)$ is thermal conductivity at a testing temperature ($W\cdot m^{-1}\cdot K^{-1}$), $\alpha(T)$ is thermal diffusivity ($mm^2\cdot s^{-1}$), $C_p(T)$ is specific heat ($J\cdot g^{-1}\cdot K^{-1}$), $\rho(T)$ is density of composite sorbent ($kg\cdot m^{-3}$).

Permeability is measured by a specially designed testing unit, which is mainly composed of testing chamber, pressure differential transmitter and rotermeter. Permeability could be determined by flow rate and pressure drop according to equation 4 and 5. Ergun model is applied for testing the permeability and no compressibility effects exist [37]. Pressure difference is tested by differential pressure meter with the error of 0.5%, and gas mass flowrate is tested by flow meter with the error of 4%. The average relative error of K is calculated, and the error of permeability is 5.08%.

$$Y = BX + \frac{1}{K} \tag{4}$$

where

$$Y = \frac{(P_{in}^{\ 2} - P_{out}^{\ 2})S}{2RT\mu m_a \Delta z}; \qquad X = \frac{m_a}{\mu S}; \qquad m_a = \rho A V_a \tag{5}$$

where K is permeability (m^2), B is shape factor, P_{in} and P_{out} are the inlet and outlet pressure of nitrogen gas, A is area of cross section (m^2), R is gas constant ($J\cdot kg^{-1}\cdot K^{-1}$), T is testing temperature (K), Δz is thickness of samples, μ and ρ are gas viscosity (Pa·s) and density ($kg\cdot m^{-3}$); m_a is mass flow rate of the gas ($kg\cdot s^{-1}$), V_a is axial velocity ($m\cdot s^{-1}$).

As for sorption characteristic of composite $SrCl_2$, the detailed testing processes could be referred to the reference [38]. The test unit is mainly composed of a sorption reactor, a refrigerant vessel, two thermostat baths, a pressure transmitter, three platinum resistance thermometers, a pressure sensor and several valves, etc. The refrigerant vessel plays a role as evaporator. Sorption capacity of composite sorbent is calculated by the refrigerant level in the vessel, which could be evaluated according to equation 6.

$$\Delta x = \frac{1}{m_{\text{sorb}}} \cdot \Delta \left\{ (1 - \frac{v'(T_e)}{v''(T_e)}) \cdot \frac{A_c}{g} \cdot \Delta P \right\} \tag{6}$$

where m_{sorb} is mass of composite $SrCl_2$ (kg), $v'(T_e)$ and $v''(T_e)$ are specific volume of saturated liquid ammonia and saturated vapor ammonia ($m^3 \cdot kg^{-1}$), A_c is the effective area of cross section of ammonia in the vessel (m^2), g is gravity acceleration (9.80 $m \cdot s^{-2}$), ΔP is pressure difference in the evaporation process (Pa).

Based on sorption capacity and time, sorption rate could be then evaluated according to equation 7.

$$v = \frac{\Delta x}{\Delta t} \tag{7}$$

Mass of composite $SrCl_2$ is measured by the balance (BS2202S) with the measuring error of 0.01 g. Pressure difference between liquid end and vapor end of the vessel is measured by smart differential pressure transmitter with a testing error of 0.2%. The relative error of sorption rate of composite sorbent is 0.92%.

4. Experimental results and discussions

4.1. Thermal diffusivity

Since novel composite $SrCl_2$ reveals similar trends in term of different densities and mass ratios of salt, representative examples with mass ratio of 50% between $SrCl_2$ and ENG as well as densities from 500 $kg \cdot m^{-3}$ to 800 $kg \cdot m^{-3}$ are selected for further illustration of thermal diffusivity, which are shown in Fig.4. Thermal diffusivities of disk and plate samples are investigated under the condition of different testing temperatures from 20°C to 100°C as shown in Fig.4a and Fig.4b, respectively. It is indicated that thermal diffusivity increases with

the decrease of testing temperature. This is mainly because higher temperature usually leads to friable structure inside composite sorbents, which results in larger thermal contact resistance. Plate samples have a higher thermal diffusivity when compared with that of disk samples. The highest thermal diffusivities of disk and plate samples are able to reach 1.96 $mm^2 \cdot s^{-1}$ and 5.66 $mm^2 \cdot s^{-1}$ at 20°C testing temperature. For different testing temperatures, thermal diffusivities of plate and disk samples range from 1.34 $mm^2 \cdot s^{-1}$ to 1.96 $mm^2 \cdot s^{-1}$ and 4.02 $mm^2 \cdot s^{-1}$ to 5.66 $mm^2 \cdot s^{-1}$, respectively.

In order to further illustrate thermal stability of novel composite $SrCl_2$ with ENG and Fe@C, disk sample with density of 500 $kg \cdot m^{-3}$ is exemplified to compare thermal diffusivities among different shot times, which is shown in Fig.5. One remarkable fact is that results among different shot times are quite close at each testing temperature when temperature increases from 20°C to 100°C. As Table 1 indicates, the equilibrium reaction temperature of $SrCl_2$ is about 96°C in term of 30°C condensation temperature, it manifests a good repeatability of thermal diffusivity in its working range.

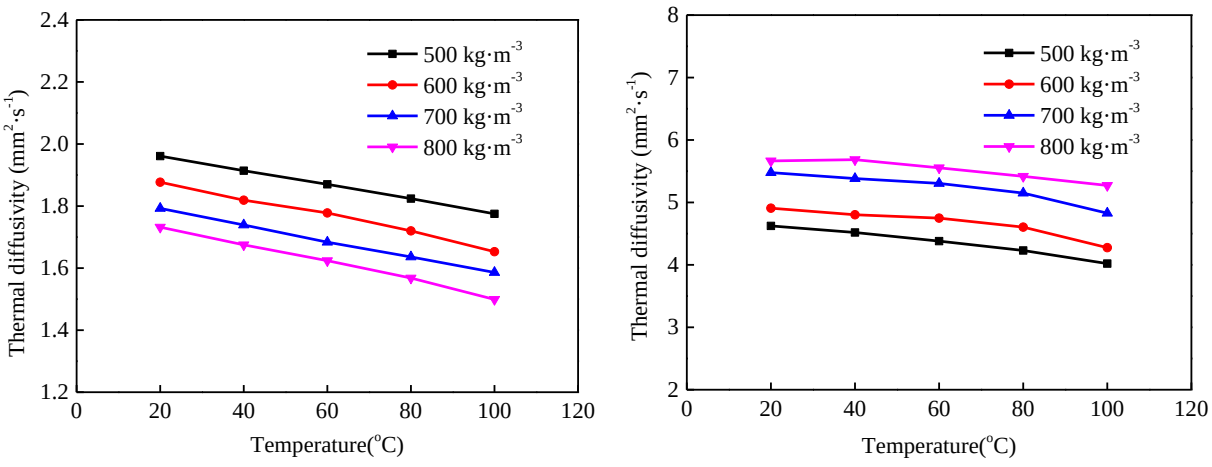

Fig.4. Thermal diffusivity of novel composite $SrCl_2$ with ENG and Fe@C vs. different testing temperatures (a) disk samples; (b) plate samples.

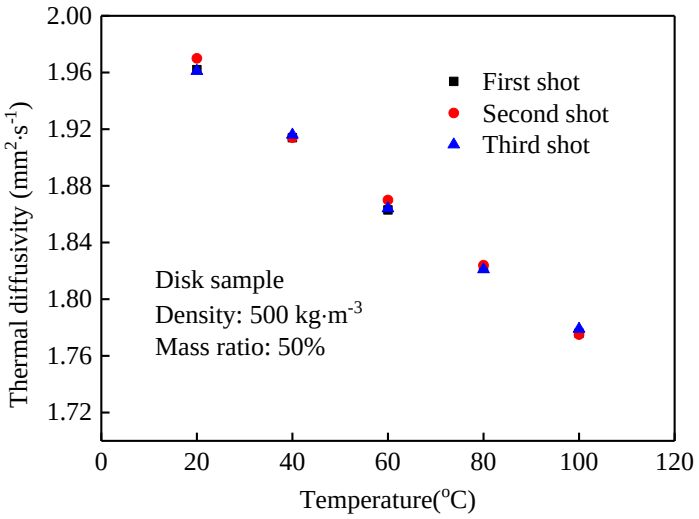

Fig.5. Thermal diffusivity of disk sample of novel composite $SrCl_2$ vs. different shot times.

In order to comprehensively evaluate thermal diffusivity, composite sorbents with different densities and mass ratios of salt are compared at 20°C testing temperature i.e. environmental temperature. Fig.6 demonstrates thermal diffusivity of novel composite $SrCl_2$ with ENG and Fe@C when densities and mass ratios range from 500 kg·m^{-3} to 800 kg·m^{-3} and from 50% to 83%, respectively. Results indicate that thermal diffusivities of disk and plate samples increase with the decrease of mass ratio. For disk sample, thermal diffusivity decreases with the increase of the density. Comparably, thermal diffusivity of plate sample shows the reverse trend. For different densities and mass ratios, thermal diffusivities of disk and plate samples range from 1.42 mm^2·s^{-1} to 1.96 mm^2·s^{-1} and 1.99 mm^2·s^{-1} to 5.66 mm^2·s^{-1}, respectively.

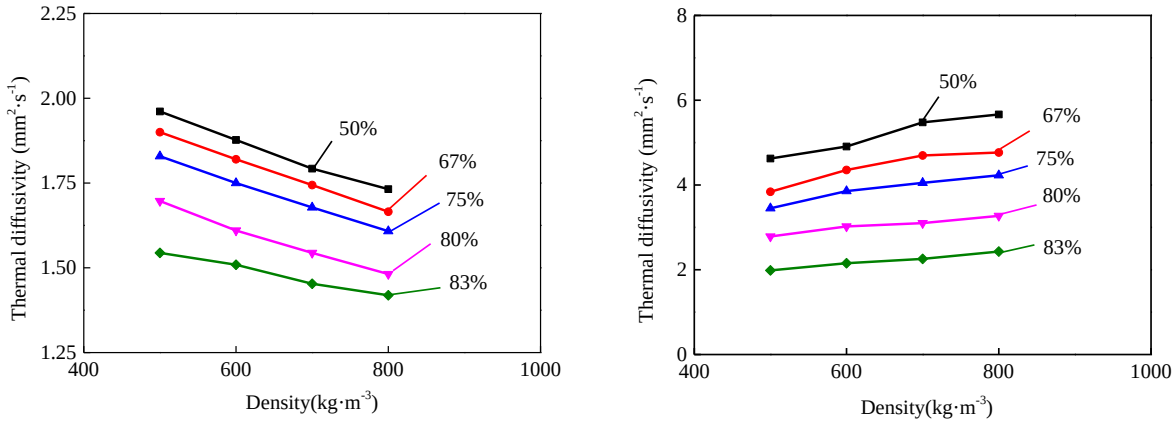

Fig.6. Thermal diffusivity of novel composite $SrCl_2$ with ENG and Fe@C vs. different densities and mass ratios of salt (a) disk samples; (b) plate samples.

4.2. Thermal conductivity

According to laser flash method, thermal conductivity of novel composite $SrCl_2$ with ENG and Fe@C could be calculated according to equation 3, in which specific heat capacity could be evaluated by equation 8. Since ratio of Fe@C accounts for quite a small part of novel composite sorbent, $SrCl_2$ and ENG will have major influences on specific heat of novel composite $SrCl_2$.

$$C_p = \beta \cdot C_{p,SrCl_2} + \gamma \cdot C_{p,ENG} + (1-\beta-\gamma) \cdot C_{p,Fe@C} \quad (8)$$

where β is mass ratio of $SrCl_2$ with respect to total mass of novel composite $SrCl_2$, γ is mass ratio of ENG with respect to total mass of novel composite $SrCl_2$.

Based on thermal diffusivity obtained at 20°C testing temperature, thermal conductivities of disk and plate samples are evaluated in term of the same densities and mass ratios of salt i.e. from 500 $kg \cdot m^{-3}$ to 800 $kg \cdot m^{-3}$ and from 50% to 83%, which are shown in Fig.7. Results demonstrate that thermal conductivity of novel composite $SrCl_2$ increases with the decrease of mass ratio of salt and the increase of the density. The highest thermal conductivities of novel composite $SrCl_2$ could reach 0.9 $W \cdot m^{-1} \cdot K^{-1}$ and 2.95 $W \cdot m^{-1} \cdot K^{-1}$ in term of disk and plate samples when density and mass ratio of salt are 800 $kg \cdot m^{-3}$ and 50%. The highest thermal conductivity of plate sample is about 14 times higher than that of granular $SrCl_2$. For different densities and mass ratios of salt, thermal conductivities of disk and plate samples range from 0.43 $W \cdot m^{-1} \cdot K^{-1}$ to 0.9 $W \cdot m^{-1} \cdot K^{-1}$ and 0.55

211 W·m^{-1}·K^{-1} to 2.95 W·m^{-1}·K^{-1}, respectively.

212

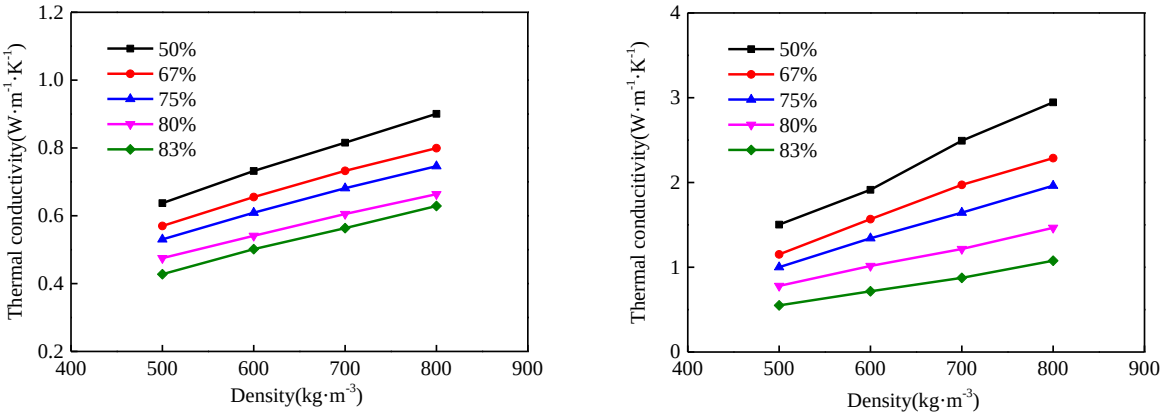

213 Fig.7. Thermal conductivity of novel composite $SrCl_2$ with ENG and Fe@C vs. different densities and mass

214 ratios (a) disk samples; (b) plate samples.

215

216 Fig.8 indicates anisotropic thermal conductivity of consolidated ENG, which could be referred to our

217 previous work [39]. One striking fact is that thermal conductivity of disk sample of consolidated composite ENG

218 first increases, then almost remains stable and decreases in the end when density of consolidated ENG increases

219 from 200 kg·m^{-3} to 780 kg·m^{-3}. Different from consolidated ENG, thermal conductivity of novel composite

220 $SrCl_2$ with ENG and Fe@C increases with the increase of density from 500 kg·m^{-3} to 800 kg·m^{-3}. The reasons

221 are elaborated as follows: For composite $SrCl_2$ with ENG and Fe@C, bulk density of ENG is much lower than

222 that of consolidated ENG. As shown in Fig.2, bulk density of ENG for composite $SrCl_2$ is no more than 400

223 kg·m^{-3}, which is still in the rising stage of thermal conductivity as shown in Fig.8. Another reason is that the

224 additives of nanoparticle and porous material will prevent the further compression of ENG since nanoparticle

225 tends to be easy to occupy the porous structure of composite sorbents. Compared with thermal conductivity of

226 disk sample, plate sample of novel composite $SrCl_2$ shows a similar trend with consolidated ENG. Thus for

composite sorbent, thermal conductivities of disk and plate sample increase with the increase of density, which are conducive to sorption reactor by using compressing technology.

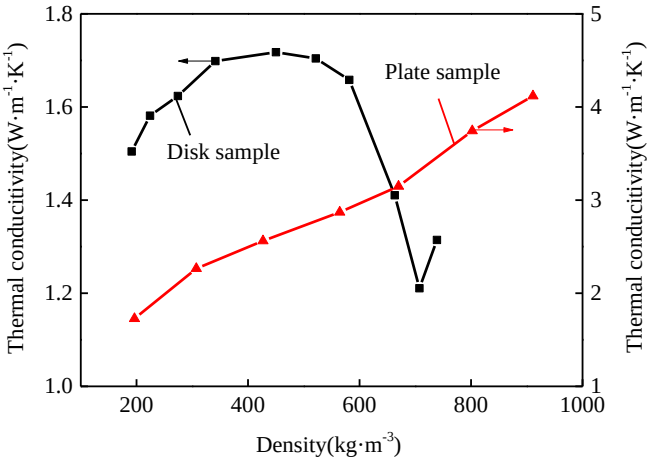

Fig.8. Anisotropic thermal conductivity of consolidated ENG [39].

Fig.9. demonstrates thermal conductivities of plate samples with different matrices in term of 500 kg·m^{-3} density, which are mutually compared for further elaboration. It is indicated that carbon coated metal will weaken the improvements of thermal conductivities by using porous materials of ENG. For composite sorbents with different carbon coated metals, thermal conductivity of sorbent with Al@C shows the best heat transfer performance whereas sorbents with Fe@C and Ni@C reveal the similar performance. Also worth noting that thermal conductivities of sorbents with different carbon coated metals become quite close when mass ratio of salt increases from 50% to 83%. This is mainly because mass ratio of ENG declines and mass ratio of salt increases, and the results are gradually close to thermal conductivity of granular salt. In order to have a comprehensive investigation of different additives, carbon coated metals and ENG are compared which are shown in Fig.10. For different densities, thermal conductivity of ENG is much higher than that of carbon coated metal, which demonstrates its positive effect on heat transfer of granular salt. Thermal conductivity of consolidated ENG is in the range from 2.55 W·m^{-1}·K^{-1} to 3.5 W·m^{-1}·K^{-1}. Compared with ENG, thermal conductivities of carbon coated metals are no more than 0.3 W·m^{-1}·K^{-1}, which are close to the value of granular salt. Al@C has a higher thermal conductivity than Ni@C and Fe@C due to the fact that density of Al@C is lower than that of other two. Ni@C and Fe@C have similar results in term of thermal conductivity.

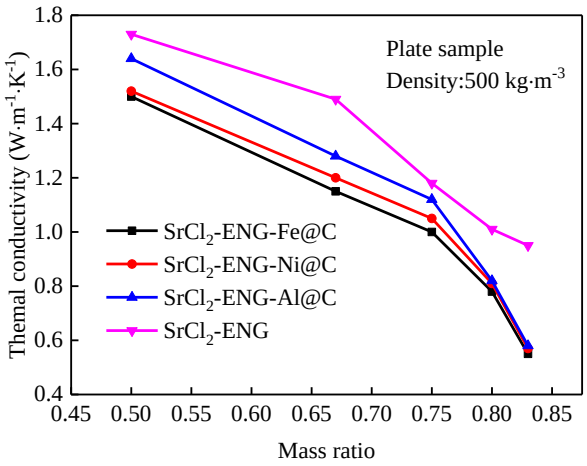

Fig.9. Thermal conductivity of composite sorbent with different matrices.

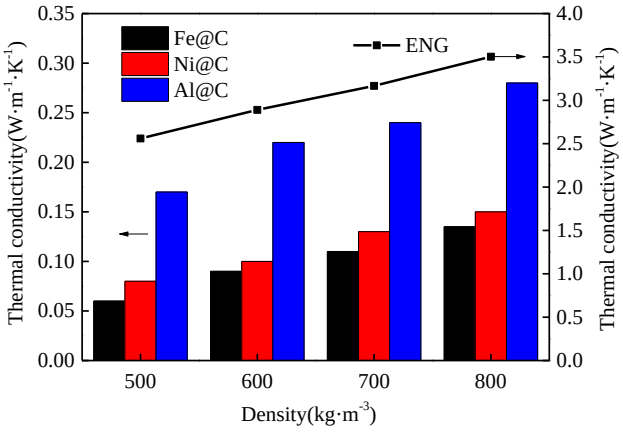

Fig.10. Comparison of thermal conductivity of different matrices.

4.3. Permeability

Table 2 shows the permeability of novel composite $SrCl_2$ with ENG and Fe@C under the condition of different densities from 400 kg·m^{-3} to 600 kg·m^{-3} and mass ratios of salt from 50% to 83%. It is worth noting that plate samples enjoy the better permeability than that of disk samples, which is similar with the results of composite sorbent with ENG and Al@C. Also worth noting that for disk and plate samples, permeabilities range from 5.4×10^{-10} m^2 to 4.5×10^{-14} m^2 and 1.2×10^{-9} m^2 to 1.5×10^{-13} m^2, respectively. Permeabilities of both disk and

plate samples increase with the decrease of density and the increase of mass ratio.

Table 2. Permeability of novel composite $SrCl_2$ with ENG and Fe@C.

Type of sorbent	Ratio/Density	400 kg·m^{-3}	500 kg·m^{-3}	600 kg·m^{-3}
Disk	50%	2.5×10^{-13} m^2	8.2×10^{-14} m^2	4.5×10^{-14} m^2
	67%	9.3×10^{-13} m^2	3.3×10^{-13} m^2	7.2×10^{-14} m^2
	75%	6.9×10^{-12} m^2	3.9×10^{-12} m^2	4.5×10^{-13} m^2
	80%	9.4×10^{-11} m^2	8×10^{-12} m^2	3.4×10^{-12} m^2
	83%	5.4×10^{-10} m^2	9.9×10^{-11} m^2	5.5×10^{-12} m^2
Plate	50%	3×10^{-12} m^2	5×10^{-13} m^2	1.5×10^{-13} m^2
	67%	4.4×10^{-12} m^2	6.5×10^{-13} m^2	3.2×10^{-13} m^2
	75%	3.8×10^{-11} m^2	6.8×10^{-12} m^2	9.8×10^{-13} m^2
	80%	6×10^{-10} m^2	4.4×10^{-11} m^2	5.8×10^{-12} m^2
	83%	1.2×10^{-9} m^2	5.5×10^{-10} m^2	2.1×10^{-11} m^2

In order to further illustrate the influence of Fe@C on composite $SrCl_2$, permeability of plate sample with Fe@C is compared with that without Fe@C when density and mass ratio are in the range from 400 kg·m^{-3} to 600 kg·m^{-3} and 50% to 83%, which is shown in Fig.11. It is noted that there exists an inflection point between mass ration of 67% and 75%. If mass ratio is lower than this point, permeability increases slightly with the increase of mass ratio. When mass ratio becomes higher, permeability of composite $SrCl_2$ will soar. Also worth noting that samples with Fe@C always enjoy a higher permeability than that without Fe@C. It is demonstrated that carbon coated metal is conducive to the improvement of mass transfer performance due to the fact that nanoparticle is easy to occupy the porous structure of composite sorbent, which further reduces a swelling and agglomeration phenomenon based on composite sorbent with ENG. Fig.12 indicates permeability of plate samples of composite $SrCl_2$ with different matrices i.e. ENG, ENG&Fe@C, ENG&Ni@C and ENG&Al@C at the density of 500 kg·m^{-3}. It is indicated that for different matrices, sorbent with Fe@C shows the highest permeability whereas sorbents without carbon coated metal displays the lowest results. Similar with thermal conductivity, permeability

of sorbents with Fe@C and Ni@C are relatively close.

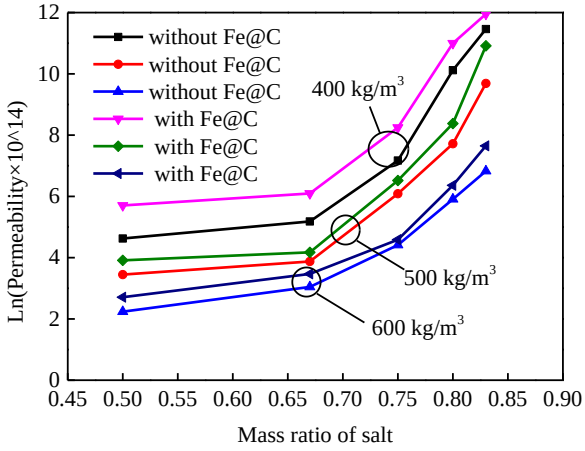

Fig.11. Permeability of plate samples of composite $SrCl_2$ with and without Fe@C vs. different mass ratios.

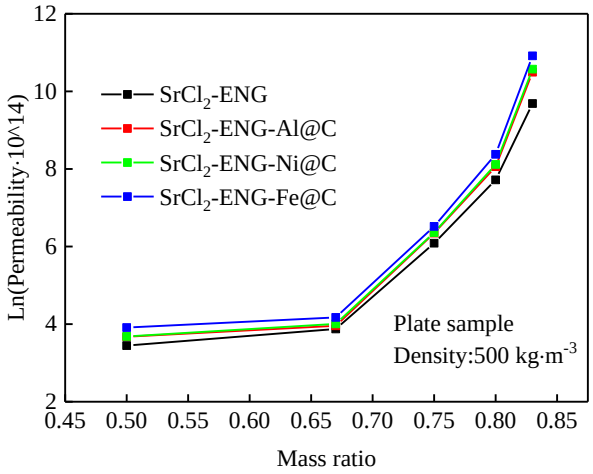

Fig.12. Permeability of plate samples of composite $SrCl_2$ with different matrices.

4.4. Sorption characteristic

Fig.13 indicates sorption rate of composite $SrCl_2$ with Fe@C and without Fe@C at different evaporation temperatures i.e. 10°C, 0°C and -10°C, and sorption temperature i.e. environmental temperature. As Fig.13a shows, when evaporation temperature is -10°C, composite sorbent with Fe@C has a faster sorption rate than that without Fe@C due to its higher mass transfer performance. One remarkable fact is that mass transfer performance becomes critical when evaporation temperature is low. Thus composite sorbent with better

permeability usually demonstrates an improved sorption performance in freezing conditions. With the increase of evaporation temperature, sorption performance of $SrCl_2$ with Fe@C and without Fe@C becomes close as shown in Fig.13b. This could be attributed to the fact that mass transfer performance of composite sorbent without Fe@C is improved with the increase of evaporation temperature, and heat transfer performance will gradually take a leading role of sorption rate. For evaporation temperature of 10°C as shown in Fig.13c, sorption rate of composite $SrCl_2$ with Fe@C and without Fe@C are almost the same which range from 0.193×10^3 kg·kg^{-1}·s^{-1} to 0.96×10^3 kg·kg^{-1}·s^{-1} due to the similar thermal conductivity. Under this scenario, carbon coated metal has a limited influence on the improvement of sorption characteristics.

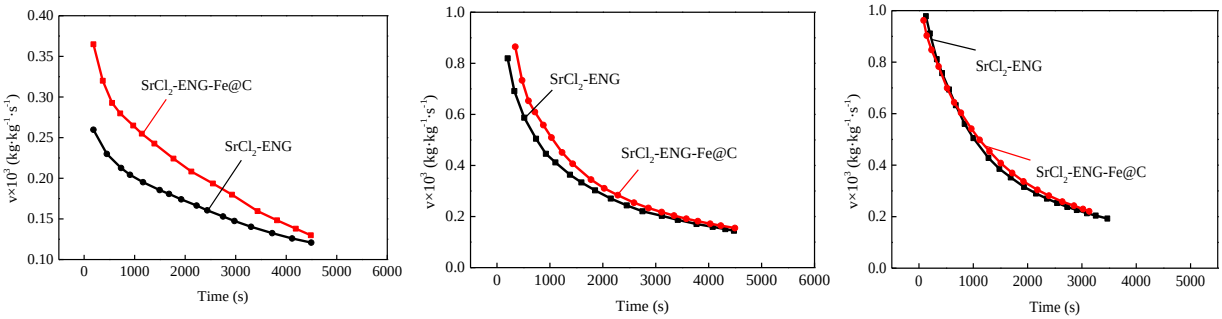

(a) (b) (c)

Fig.13. Sorption reaction rate of composite $SrCl_2$ with and without Fe@C vs different evaporation temperatures (a) -10°C; (b) 0°C; (c) 10°C;

In order to have comprehensive investigation, composite sorbents with several typical kinds of matrices are summarized and compared in terms of thermal conductivity, permeability and cost per kilogram sorbent, which are shown in Table 3. Mass ratio between salt and matrix is 75% and density is around 500 kg·m^{-3}. $CaCl_2$ and $SrCl_2$ are selected as representative sorbents due to their similar properties. One striking fact is that MWCNT is not suitable for developing composite sorbent due to its remarkably high cost. It is worth noting that composite sorbent by adding ENG-TSA usually has the highest thermal conductivity whereas it shows the lowest permeability. Thus ENG-TSA could be a possible candidate for sorption system if mass transfer is not required that high, e.g. evaporation temperature is above 0°C. For conventional sorption chiller, ENG is still a good choice due to the reasonable heat and mass transfer performance. If sorption system is applied for both air conditioning and freezing condition, composite sorbents with ENG and carbon coated metal will take an improved effect for the system e.g. sorption freezer or sorption heat pump at a low environmental temperature.

The additional cost by adding carbon coated metal could be accepted, which is no more than 20% when compared with that using ENG. The cost difference by using ENG with and without carbon coated metal in Table 3 is mainly due to the difference from cost of granular $CaCl_2$ and $SrCl_2$.

Table 3. General comparison among common composite sorbents by using different matrices.

Composite sorbent	Density ($kg \cdot m^{-3}$)	Thermal conductivity ($W \cdot m^{-1} \cdot K^{-1}$)	Permeability (m^2)	Cost ($CNY \cdot kg^{-1}$)	Ref.
$CaCl_2$/ENG	550	1.36	4×10^{-12}	78	[24]
$CaCl_2$/ENG-TSA	500	27.1	7.3×10^{-13}	320	[28]
$CaCl_2$/MWCNT	-	1.52	-	2000	[30]
$CaCl_2$/GF	-	0.57	-	550	[40]
$SrCl_2$/ENG&Al@C	500	1.12	5.1×10^{-12}	160	[41]
$SrCl_2$/ENG&Ni@C	500	1.05	5.8×10^{-12}	152	[42]
$SrCl_2$/ENG&Fe@C	500	1	6.8×10^{-12}	154	Present study

5. Conclusions

Novel composite $SrCl_2$ is developed with ENG and Fe@C as the additive to improve heat and mass transfer performance. Anisotropic thermal conductivity and permeability of the samples are investigated and compared with that by using different carbon coated metals. Sorption characteristic is also investigated for further elaboration based on heat and mass transfer performance. Conclusions are yielded as follows:

[1] Thermal diffusivity increases with the decrease of testing temperature and the decrease of mass ratio. For different densities and mass ratios of salt, thermal diffusivities of disk and plate samples range from 1.42 $mm^2 \cdot s^{-1}$ to 1.96 $mm^2 \cdot s^{-1}$ and 1.99 $mm^2 \cdot s^{-1}$ to 5.66 $mm^2 \cdot s^{-1}$. The highest thermal conductivities of novel composite $SrCl_2$ with ENG and Fe@C could reach 0.9 $W \cdot m^{-1} \cdot K^{-1}$ and 2.95 $W \cdot m^{-1} \cdot K^{-1}$ in term of disk and plate samples when density and mass ratio are 800 $kg \cdot m^{-3}$ and 50%. For different densities and mass ratios of salt, thermal conductivities of disk and plate samples range from 0.43 $W \cdot m^{-1} \cdot K^{-1}$ to 0.9 $W \cdot m^{-1} \cdot K^{-1}$ and 0.55 $W \cdot m^{-1} \cdot K^{-1}$ to 2.95 $W \cdot m^{-1} \cdot K^{-1}$, respectively.

[2] Thermal conductivity of compact ENG is in the range from 2.55 $W \cdot m^{-1} \cdot K^{-1}$ to 3.5 $W \cdot m^{-1} \cdot K^{-1}$. Compared with ENG, thermal conductivity of carbon coated metal is no more than 0.3 $W \cdot m^{-1} \cdot K^{-1}$, which is close to the value of granular salt. Al@C has the higher thermal conductivity than Ni@C and

Fe@C whereas Ni@C and Fe@C have the similar thermal conductivity.

[3] For disk and plate samples permeabilities range from 5.4×10^{-10} m^2 to 4.5×10^{-14} m^2 and 1.2×10^{-9} m^2 to 1.5×10^{-13} m^2, respectively. Permeability increases with the decrease of density and the increase of mass ratio in term of disk and plate samples. For different matrices, sorbent with Fe@C shows the highest thermal permeability whereas sorbents without carbon coated metal reveals the lowest results. Permeabilities of the sorbents with Fe@C and Ni@C are similar.

[4] Considering sorption characteristic of composite sorbents, sorption reaction rate is mainly determined by mass transfer performance when evaporation temperature is -10°C, and composite sorbent with Fe@C has a faster sorption reaction rate than that without Fe@C. With the increase of evaporation temperature, sorption rate of composite $SrCl_2$ with Fe@C and without Fe@C become close. When evaporation temperature is 10°C, sorption rates of composite $SrCl_2$ with Fe@C and without Fe@C are almost the same.

With potentially wide use of nanoparticles for material improvement in various fields of energy conversion technologies e.g. absorption refrigeration and chemical heat pump, composite sorbent with ENG and carbon coated metal could be considered as a method to modify the performance of sorption system in terms of different energy demands. It takes an advantage especially for the place with relatively low environmental temperature, which further broadens temperature application range of sorption system when compared with vapor compression system.

Acknowledgements

This research was supported by National Natural Science Foundation of China under contract number (51606118), Innovative Research Groups under contract number (51521004) and Heat-STRESS project (EP/N02155X/1) funded by the Engineering and Physical Science Research Council of the UK.

References

[1] A. Freni, G. Maggio, A. Sapienza, A. Frazzica, G. Restuccia, S. Vasta, Comparative analysis of promising adsorbent/adsorbate pairs for adsorptive heat pumping, air conditioning and refrigeration, Applied Thermal Engineering, 104 (2016) 85-95.

[2] F.B. Cortés, F. Chejne, F. Carrasco-Marín, A.F. Pérez-Cadenas, C. Moreno-Castilla, Water sorption on silica- and zeolite-supported hygroscopic salts for cooling system applications, Energy Conversion and Management, 53(1) (2012) 219-223.

[3] A. Pal, K. Thu, S. Mitra, I.I. El-Sharkawy, B.B. Saha, H.-S. Kil, S.-H. Yoon, J. Miyawaki, Study on biomass derived activated carbons for adsorptive heat pump application, International Journal of Heat and Mass Transfer, 110 (2017) 7-19.

[4] B. Dawoud, Y. Aristov, Experimental study on the kinetics of water vapor sorption on selective water sorbents, silica gel and alumina under typical operating conditions of sorption heat pumps, International Journal of Heat and Mass Transfer, 46(2) (2003) 273-281.

[5] L. Jiang, L.W. Wang, X.F. Zhang, C.Z. Liu, R.Z. Wang, Performance prediction on a resorption cogeneration cycle for power and refrigeration with energy storage, Renewable Energy, 83 (2015) 1250-1259.

[6] L. Jiang, L. Wang, A.P. Roskilly, R. Wang, Design and performance analysis of a resorption cogeneration system, International Journal of Low-Carbon Technologies, 8 (2013) 85-91.

[7] H. Liu, K. Nagano, Numerical simulation of an open sorption thermal energy storage system using composite sorbents built into a honeycomb structure, International Journal of Heat and Mass Transfer, 78 (2014) 648-661.

[8] L. Jiang, L. Wang, R. Wang, F. Zhu, Y. Lu, A.P. Roskilly, Experimental investigation on an innovative resorption system for energy storage and upgrade, Energy Conversion and Management, 138 (2017) 651-658.

[9] R. Zhao, S. Deng, Y. Liu, Q. Zhao, J. He, L. Zhao, Carbon pump: Fundamental theory and applications, Energy, 119 (2017) 1131-1143.

[10] K. Thu, B.B. Saha, K.J. Chua, K.C. Ng, Performance investigation of a waste heat-driven 3-bed 2-evaporator adsorption cycle for cooling and desalination, International Journal of Heat and Mass Transfer, 101 (2016) 1111-1122.

[11] A. Freni, L. Bonaccorsi, L. Calabrese, A. Caprì, A. Frazzica, A. Sapienza, SAPO-34 coated adsorbent heat exchanger for adsorption chillers, Applied Thermal Engineering, 82 (2015) 1-7.

[12] T.M. Yurieva, L.M. Plyasova, O.V. Makarova, T.A. Krieger, Mechanisms for hydrogenation of acetone to isopropanol and of carbon oxides to methanol over copper-containing oxide catalysts, Journal of Molecular Catalysis A: Chemical, 113(3) (1996) 455-468.

[13] Y.I. Aristov, Adsorptive transformation and storage of renewable heat: Review of current trends in adsorption dynamics, Renewable Energy, 110 (2017) 105-114.

[14] A. Li, K. Thu, A.B. Ismail, M.W. Shahzad, K.C. Ng, Performance of adsorbent-embedded heat exchangers using binder-coating method, International Journal of Heat and Mass Transfer, 92 (2016) 149-157.

[15] R.E. Critoph, L. Turner, Heat transfer in granular activated carbon beds in the presence of adsorbable gases, International Journal of Heat and Mass Transfer, 38(9) (1995) 1577-1585.

[16] Y.D. Tu, R.Z. Wang, L.J. Hua, T.S. Ge, B.Y. Cao, Desiccant-coated water-sorbing heat exchanger: Weakly-coupled heat and mass transfer, International Journal of Heat and Mass Transfer, 113 (2017) 22-31.

[17] Y.J. Zhao, L.W. Wang, R.Z. Wang, K.Q. Ma, L. Jiang, Study on consolidated activated carbon: Choice of optimal adsorbent for refrigeration application, International Journal of Heat and Mass Transfer, 67 (2013) 867-876.

[18] J.V. Veselovskaya, M.M. Tokarev, A.D. Grekova, L.G. Gordeeva, Novel ammonia sorbents ‘‘porous matrix

403 modified by active salt" for adsorptive heat transformation: 6. The ways of adsorption dynamics enhancement,
404 Applied Thermal Engineering, 37 (2012) 87-94.
405 [19] Y.I. Aristov, G. Restuccia, M.M. Tokarev, H.D. Buerger, A. Freni, Selective Water Sorbents for Multiple
406 Applications. 11. $CaCl_2$ Confined to Expanded Vermiculite, Reaction Kinetics and Catalysis Letters, 71(2) (2000)
407 377-384.
408 [20] L. Dongliang, P. Hao, L. Deqing, Thermal conductivity enhancement of clathrate hydrate with nanoparticles,
409 International Journal of Heat and Mass Transfer, 104 (2017) 566-573.
410 [21] S. Biloé, S. Mauran, Gas flow through highly porous graphite matrices, Carbon, 41(3) (2003) 525-537.
411 [22] Z. Tamainot-Telto, R.E. Critoph, Thermophysical properties of monolithic carbon, International Journal of
412 Heat and Mass Transfer, 43(11) (2000) 2053-2058.
413 [23] Z. Tamainot-Telto, R.E. Critoph, Monolithic carbon for sorption refrigeration and heat pump applications,
414 Applied Thermal Engineering, 21(1) (2001) 37-52.
415 [24] L. Jiang, L.W. Wang, Z.Q. Jin, B. Tian, R.Z. Wang, Permeability and thermal conductivity of compact
416 adsorbent of salts for sorption refrigeration, Journal of heat transfer ASME, 134 (2012) 104503-104506.
417 [25] L. Jiang, L.W. Wang, Z.Q. Jin, R.Z. Wang, Y.J. Dai, Effective thermal conductivity and permeability of
418 compact compound ammoniated salts in the adsorption/desorption process, International Journal of Thermal
419 Sciences, 71 (2013) 103-110.
420 [26] S.R. Dhakate, S. Sharma, M. Borah, R.B. Mathur, T.L. Dhami, Expanded graphite-based electrically
421 conductive composites as bipolar plate for PEM fuel cell, International Journal of Hydrogen Energy, 33(23)
422 (2008) 7146-7152.
423 [27] A. Celzard, M. Krzesiñska, J.F. Marêché, S. Puricelli, Scalar and vectorial percolation in compressed
424 expanded graphite, Physica A: Statistical Mechanics and its Applications, 294(3–4) (2001) 283-294.

425 [28] L. Jiang, L.W. Wang, R.Z. Wang, Investigation on thermal conductive consolidated composite $CaCl_2$ for
426 adsorption refrigeration, International Journal of Thermal Sciences, 81 (2014) 68-75.
427 [29] Y.N. Zhang, R.Z. Wang, Y.J. Zhao, T.X. Li, S.B. Riffat, N.M. Wajid, Development and thermochemical
428 characterizations of vermiculite/SrBr2 composite sorbents for low-temperature heat storage, Energy, 115, Part 1
429 (2016) 120-128.
430 [30] T. Yan, T.X. Li, R.Z. Wang, R. Jia, Experimental investigation on the ammonia adsorption and heat transfer
431 characteristics of the packed multi-walled carbon nanotubes, Applied Thermal Engineering, 77 (2015) 20-29.
432 [31] T. Yan, T.X. Li, H. Li, R.Z. Wang, Experimental study of the ammonia adsorption characteristics on the
433 composite sorbent of CaCl2 and multi-walled carbon nanotubes, International Journal of Refrigeration, 46 (2014)
434 165-172.
435 [32] C. Lei, S. He, Z. Du, F. Pan, Q. Zhu, H. Li, Effects of gas composition and temperature on the fluidization
436 characteristics of carbon-coated iron ore, Powder Technology, 301 (2016) 608-614.
437 [33] C. Vales-Pinzon, R.A. Medina-Esquivel, J. Ordonez-Miranda, J.J. Alvarado-Gil, Thermal transfer in
438 mixtures of ethylene glicol with carbon coated iron nanoparticles under the influence of a uniform magnetic field,
439 Journal of Alloys and Compounds, 643, Supplement 1 (2015) S71-S74.
440 [34] L. Jiang, Y.J. Lu, K. Tang, Y.D. Wang, R. Wang, A.P. Roskilly, L. Wang, Investigation on heat and mass
441 transfer performance of novel composite strontium chloride for sorption reactors, Applied Thermal Engineering,
442 121 (2017) 410-418.
443 [35] Z. Jin, B. Tian, L. Wang, R. Wang, Comparison on Thermal Conductivity and Permeability of Granular and
444 Consolidated Activated Carbon for Refrigeration, Chinese Journal of Chemical Engineering, 21(6) (2013)
445 676-682.
446 [36] Q. Wu, X. Yu, H. Zhang, Y. Chen, L. Liu, X. Xie, K. Tang, Y. Lu, Y. Wang, A.P. Roskilly, Fabrication and

447 thermal conductivity improvement of novel composite adsorbents adding with nanoparticles, Chinese journal of
448 mechanical engineering, 6 (2016) 1114-1118.
449 [37] L.W. Wang, S.J. Metcalf, R.E. Critoph, Z. Tamainot-Telto, R. Thorpe, Two types of natural graphite host
450 matrix for composite activated carbon adsorbents, Applied Thermal Engineering, 50(2) (2013) 1652-1657.
451 [38] L. Jiang, J. Gao, L. Wang, R. Wang, Y. Lu, A.P. Roskilly, Investigation on performance of multi-salt
452 composite sorbents for multilevel sorption thermal energy storage, Applied Energy, 190 (2017) 1029-1038.
453 [39] L.W. Wang, Z. Tamainot-Telto, S.J. Metcalf, R.E. Critoph, R.Z. Wang, Anisotropic thermal conductivity and
454 permeability of compacted expanded natural graphite, Applied Thermal Engineering, 30(13) (2010) 1805-1811.
455 [40] K. Fayazmanesh, S. Salari, M. Bahrami, Effective thermal conductivity modeling of consolidated sorption
456 composites containing graphite flakes, International Journal of Heat and Mass Transfer, 115 (2017) 73-79.
457 [41] L. Jiang, Y.J. Lu, K. Tang, Y.D. Wang, R. Wang, A.P. Roskilly, L. Wang, Investigation on heat and mass
458 transfer performance of novel composite strontium chloride for sorption reactors, Applied Thermal Engineering,
459 121(Supplement C) (2017) 410-418.
460 [42] L. Jiang, R.Z. Wang, Y.J. Lu, A.P. Roskilly, L.W. Wang, K. Tang, Investigation on innovative thermal
461 conductive composite strontium chloride for ammonia sorption refrigeration, International Journal of
462 Refrigeration, 85(Supplement C) (2018) 157-166.
463